

Insights Into Flexoelectric Solids From Strain-Gradient Elasticity

Sheng Mao

Department of Mechanical Engineering
and Applied Mechanics,
University of Pennsylvania,
Philadelphia, PA 19104
e-mail: maosheng@seas.upenn.edu

Prashant K. Purohit¹

Department of Mechanical Engineering
and Applied Mechanics,
University of Pennsylvania,
Philadelphia, PA 19104
e-mail: purohit@seas.upenn.edu

A material is said to be flexoelectric when it polarizes in response to strain gradients. The phenomenon is well known in liquid crystals and biomembranes but has received less attention in hard materials such as ceramics. Here we derive the governing equations for a flexoelectric solid under small deformation. We assume a linear constitutive relation and use it to prove a reciprocal theorem for flexoelectric materials as well as to obtain a higher-order Navier equation in the isotropic case. The Navier equation is similar to that in Mindlin's theory of strain-gradient elasticity. We also provide analytical solutions to several boundary value problems. We predict size-dependent electromechanical properties and flexoelectric modulation of material behavior. Our results can be used to interpret experiments on flexoelectric materials which are becoming increasingly sophisticated due to the advent of nanoscale probes. [DOI: 10.1115/1.4027451]

1 Introduction

Coupled electromechanical phenomena are common in nature. For example, strains can be generated in dielectrics by the application of electric fields through electrostriction. Strains can also be generated in a special class of dielectrics by the phenomenon of piezoelectricity. Conversely, a piezoelectric material can be polarized when a stress is applied on it. The study of these phenomena has a long history in mechanics of materials and has been documented in quite a number of texts, including those of Landau et al. [1], Maugin and Eringen [2], Kovetz [3], and many others.

A lesser known phenomenon, termed flexoelectricity, is the coupling between polarization and strain gradient (SG). It was extensively studied in liquid crystals starting from the 1960s [4,5] and has been extended recently to lipid bilayer membranes [6–9]. During this period, it was known that a coupling between polarization and strain gradient exists also in hard materials, even those with centrosymmetric lattices [10–13]. But, unlike soft materials (like liquid crystals and biomembranes), it has been difficult to measure flexoelectric constants in hard materials because very large strain gradients are required to produce measurable effects in macroscopic specimens. In the last decade, this problem has been circumvented by studying thin films of ceramic materials and using nanoscale probes to measure polarizations and strains. As a result, there has been a revival of interest in flexoelectricity. Flexoelectric constants have been directly measured in several materials with high dielectric susceptibility [14–17]. It has been suggested that flexoelectricity in nanoscale thin films leads to an enhanced piezoelectric response [18,19]. As noted in Ref. [20], “flexoelectricity is not just a substitute for piezoelectricity at the nanoscale; it also enables additional electromechanical functionalities not available otherwise.” For example, the flexoelectric effect is implicated in polarization rotations in ferroelectrics [21] and size-dependent material properties [22–26] in some ceramics. Here, we show how stress concentration factors (SCF) in flexoelectric solids can be modulated by applied electric fields.

Early theoretical treatment of flexoelectricity focused primarily on its microscopic origins. A rigid-ion model was proposed by Tagantsev [27] and was recently developed by Ref. [28]. In this model, flexoelectricity arises as a result of broken lattice symmetry. Later, the study of graphene [29] showed that electron redistribution is also an important source of flexoelectricity. The electronic contribution to flexoelectricity was studied in detail by

Ref. [30,31] and Ref. [32] attempted a first-principles calculation of flexoelectric constants of BaTiO₃. These and other topics have been discussed in a review [33] where we have shed light on the developments in the field over the last few decades.

Despite these developments, there are only a few papers in which a continuum-based framework for flexoelectricity is utilized to solve boundary value problems (BVPs). One such paper is that of Majdoub et al. [22,23] who studied a flexoelectric cantilever beam, accounting for both piezoelectric and flexoelectric effects. They showed that the piezoelectric effect in BaTiO₃ is enhanced due to flexoelectricity and verified the predictions of their continuum model by performing molecular simulations. Recently, [34] generalized their results to clamped–clamped and simply supported beams. In these papers, the contribution of flexoelectricity is summarized by a single constant. While this is sufficient for a one-dimensional beam problem, these solutions can only provide limited information about the full fourth-order flexoelectric tensor. For this reason, we need to analyze flexoelectric boundary value problems in two and three dimensions.

In general, electromechanical problems can be solved by combining the governing equations of electrostatics and continuum mechanics [3,35]. As a special case, linear elasticity and electrostatics suffice to solve boundary value problems for piezoelectric solids. However, flexoelectricity involves strain gradients, so we need to invoke theories of strain-gradient elasticity (SGE). The field of SGE was developed mainly by Toupin [36], Koiter [37], and Mindlin [38–40] to understand size-dependent phenomena in solids and has led to a number of “nonlocal” theories of elasticity and plasticity [41–44]. In these theories, the energy density depends both on the strain and its gradient, so in addition to the usual elastic constants, several material length scales enter into the constitutive laws. A common feature of all these theories is the nonsymmetry of the true stress tensor, and the existence of couple and higher-order stresses. In each theory, the higher-order stresses depend on different components of the double displacement gradient [45,46]. This variation is also apparent in the literature on flexoelectricity [17,22,23,27,47]. Here, we adopt a widely studied SGE model for isotropic materials [48] which is based on the general strain-gradient tensor.

In the sequel, we first combine a theory of SGE and classical electrostatics to derive the governing equations and boundary conditions (BCs) for general flexoelectric dielectrics. Second, we propose a linear constitutive law and prove a reciprocal theorem. Third, we restrict ourselves to the study of isotropic materials and derive the governing Navier equation for the problem. Last, we use this machinery to solve a few BVPs, including beam bending and axisymmetric plane problems. Our solutions can be used to

¹Corresponding author.

Manuscript received March 27, 2014; final manuscript received April 2, 2014; accepted manuscript posted April 18, 2014; published online May 5, 2014. Assoc. Editor: Pradeep Sharma.

interpret experiments on flexoelectric solids and can also provide a benchmark for verifying continuum-based computational methods for solving flexoelectric boundary value problems.

2 Governing Equations

Consider an elastic dielectric body occupying region V with a boundary ∂V in three-dimensional space. Without loss of generality, we will develop our theory in a Cartesian coordinate system with orthonormal basis $\{\mathbf{e}_1, \mathbf{e}_2, \mathbf{e}_3\}$ and respective coordinates $\{x_1, x_2, x_3\}$. The displacement field in the body is $u(x_1, x_2, x_3)$. The infinitesimal strain tensor is defined as

$$S_{ij} = \frac{1}{2}(u_{i,j} + u_{j,i}) \quad (1)$$

Here, we use the notation a_i to denote the i th component of vector a . $a_{i,j}$ (same as $\partial_j a_i$) is a shorthand of $\partial a_i / \partial x_j$. The same rules apply to second and higher-order tensors. Hence, we write the strain gradients as $S_{jk,i}$. We give only a concise summary of the governing equations since these can be found elsewhere [38,43,44,48,49]. The work conjugate of the strain S_{ij} is the stress T_{ij} . Similarly, the work conjugate of the strain gradient $S_{jk,i}$ is the third-order stress \hat{T}_{ijk} . Consequently, there is an additional term in the equilibrium equation

$$T_{jk,j} - \hat{T}_{ijk,ij} + b_k = 0 \quad (2)$$

where b_k is the body force.

According to classical electrostatics, in a dielectric there are three relevant fields—the electric field E_i , the electric displacement D_i and the polarization field P_i . These three quantities are related to each other through

$$D_i = \epsilon_0 E_i + P_i \quad (3)$$

where ϵ_0 is the permittivity of vacuum. The electric field is the negative gradient of a scalar potential φ , so that $E_i = -\varphi_{,i}$. In a dielectric body, there is no free charge, so from the Maxwell equations

$$D_{i,i} = -\epsilon_0 \varphi_{,ii} + P_{i,i} = 0 \quad (4)$$

This equation, along with Eq. (2) constitutes the governing equation of a general dielectric with SG effects, under small deformations. These governing equations admit six types of BCs as follows:

- (1) displacement boundary condition

$$u_i = \tilde{u}_i, \quad \text{on } \partial V_u \quad (5)$$

- (2) normal derivative boundary condition

$$u_{i,j} n_j = \tilde{v} \quad \text{on } \partial V_v \quad (6)$$

- (3) traction boundary condition

$$n_j (T_{jk} - \hat{T}_{ijk,i}) - D_j^n n_i \hat{T}_{ijk} - (D_p^n n_p) n_i n_j \hat{T}_{ijk} = \tilde{t}_k, \quad \text{on } \partial V_t \quad (7)$$

- (4) higher-order traction boundary condition

$$n_i n_j \hat{T}_{ijk} = \tilde{r}_k \quad \text{on } \partial V_r \quad (8)$$

- (5) potential boundary condition

$$\varphi = \tilde{\varphi} \quad \text{on } \partial V_\varphi \quad (9)$$

- (6) surface charge boundary condition

$$n_i D_i = -\tilde{\omega} \quad \text{on } \partial V_D \quad (10)$$

In the above n_i is the unit normal, \tilde{v} means that v is prescribed (so also for the other prescribed quantities \tilde{r}, \tilde{u} , etc.), and $D_j^n = \partial_j - n_j n_k \partial_k$ is the surface gradient operator. For the BVP to be well posed we require $\partial V_\varphi \cup \partial V_D = \partial V_u \cup \partial V_t = \partial V_v \cup \partial V_r = \partial V$ and $\partial V_\varphi \cap \partial V_D = \partial V_u \cap \partial V_t = \partial V_v \cap \partial V_r = \emptyset$.

3 Constitutive Laws and a Reciprocal Theorem

So far, we have given the governing equations for a linear electromechanical theory of dielectrics with SG effects. For such a material, the stored energy density W is of the form

$$W(S_{ij}, S_{jk,i}, D_i) = W^L(S_{ij}, S_{jk,i}, P_i) + \frac{1}{2} \epsilon_0 E_i E_i \quad (11)$$

Following Toupin [50], we will work with W^L . Flexoelectric materials, as concerned now, are in the class in which W^L is quadratic

$$W^L(S_{ij}, S_{jk,i}, P_i) = \frac{1}{2} c_{ijkl} S_{ij} S_{kl} + \frac{1}{2} a_{ij} P_i P_j + d_{ijk} S_{ij} P_i + f_{ijkl} S_{jk,i} P_l + \frac{1}{2} h_{ijklmn} S_{jk,i} S_{mn,l} \quad (12)$$

where c_{ijkl} is the elasticity tensor, d_{ijk} is the piezoelectric tensor, f_{ijkl} is the flexoelectric tensor, a_{ij} is the reciprocal susceptibility tensor and h_{ijklmn} is the strain-gradient elasticity tensor. By use of Toupin's variational principles [50], we obtain the constitutive laws for a flexoelectric material

$$\frac{\partial W^L}{\partial S_{ij}} = T_{ij} = c_{ijkl} S_{kl} + d_{ijk} P_k \quad (13)$$

$$\frac{\partial W^L}{\partial S_{jk,i}} = \hat{T}_{ijk} = f_{ijkl} P_l + h_{ijklmn} S_{mn,l} \quad (14)$$

$$\frac{\partial W^L}{\partial P_i} = E_i = a_{ij} P_j + d_{ijl} S_{ij} + f_{ijkl} S_{jk,i} \quad (15)$$

Using the governing equations and the linear constitutive relations above, we prove a reciprocal theorem as follows. Consider the solutions to two different problems, the original problem (problem 1) and the reciprocal problem (problem 2) which we differentiate by upper indices 1 and 2. The total work done by the original quantities through their reciprocal conjugates is

$$\mathcal{W}^{(12)} = \int_V [T_{ij}^{(1)} S_{ij}^{(2)} + \hat{T}_{ijk}^{(1)} S_{jk,i}^{(2)} + E_i^{(1)} D_i^{(2)}] dv \quad (16)$$

$\mathcal{W}^{(21)}$, which is the work done by the reciprocal quantities through their original conjugates can be defined in a similar manner. Applying integration by parts and using the boundary conditions, we obtain

$$\mathcal{W}^{(12)} = \int_V [-(T_{jk}^{(1)} - \hat{T}_{ijk,i}^{(1)})_j u_k^{(2)} + \varphi^{(1)} D_{i,i}^{(2)}] dv + \int_{\partial V} [t_i^{(1)} u_i^{(2)} + r_i^{(1)} v_i^{(2)} + \varphi^{(1)} \omega^{(2)}] ds \quad (17)$$

Plugging in the governing Eqs. (2) and (4), we get

$$\mathcal{W}^{(12)} = \int_V [b_k^{(1)} u_k^{(2)}] dv + \int_{\partial V} [t_i^{(1)} u_i^{(2)} + r_i^{(1)} v_i^{(2)} + \varphi^{(1)} \omega^{(2)}] ds \quad (18)$$

Thus, $\mathcal{W}^{(12)}$ is completely determined by the body force and boundary loads. Alternatively, $\mathcal{W}^{(12)}$ can also be written by use of the constitutive laws

$$\mathcal{W}^{(12)} = \int_V \left[c_{ijkl} S_{kl}^{(2)} S_{ij}^{(1)} + a_{ij} P_i^{(2)} P_j^{(1)} + \varepsilon_0 E_i^{(2)} E_i^{(1)} + d_{ijk} (P_k^{(2)} S_{ij}^{(1)} + P_k^{(1)} S_{ij}^{(2)}) + f_{ijkl} (P_l^{(2)} S_{jk,i}^{(1)} + P_l^{(1)} S_{jk,i}^{(2)}) \right] dv \quad (19)$$

Due to Maxwell relations c_{ijkl} and a_{ij} have major symmetry, hence $\mathcal{W}^{(12)}$ is symmetric with respect to its upper indices. In other words

$$\mathcal{W}^{(12)} = \mathcal{W}^{(21)} \quad (20)$$

Writing the above equation in the form of Eq. (18) proves the reciprocal theorem. Furthermore, in the absence of body force and higher-order traction, the reciprocal theorem can be written in a compact form

$$\int_{\partial V} [t_i^{(1)} u_i^{(2)} + \varphi^{(1)} \omega^{(2)}] ds = \int_{\partial V} [t_i^{(2)} u_i^{(1)} + \varphi^{(2)} \omega^{(1)}] ds \quad (21)$$

An example to demonstrate this result will be shown later in the paper.

4 Isotropic Flexoelectric Material

The tensorial nature of the constitutive laws implies a rich variety of flexoelectric materials. However, in order to understand the general features of a flexoelectric material, we must first study the simplest materials in this class. Therefore, we specialize to an isotropic flexoelectric material. Isotropic materials cannot be piezoelectric, so $d_{ijk} = 0$. Furthermore, for an isotropic material, the fourth-order tensors c_{ijkl} and f_{ijkl} both have only two independent constants and the reciprocal susceptibility tensor a_{ij} has only one. For the treatment of SGE in an isotropic material, we follow Aravas [48] who introduces one additional material length scale l . As a result, our stored energy density W^L takes the simplified form

$$W^L = \frac{1}{2} \lambda S_{ii} S_{jj} + \mu S_{ij} S_{ij} + \frac{1}{2} l^2 (\lambda S_{kk,i} S_{ll,i} + 2\mu S_{jk,i} S_{jk,i}) + \frac{1}{2} a P_i P_j + (f_1 S_{kk,i} P_i + 2f_2 S_{ij,i} P_j) \quad (22)$$

where λ and μ are Lamé constants and f_1 and f_2 are two flexoelectric constants. a is the reciprocal susceptibility which is related to the dielectric permittivity ε and susceptibility χ through $a^{-1} = \varepsilon_0 \chi = \varepsilon - \varepsilon_0$. The above isotropic assumption leads to the following constitutive relations:

$$T_{ij} = \lambda S_{kk} \delta_{ij} + 2\mu S_{ij} \quad (23)$$

$$\hat{T}_{ijk} = (\lambda S_{pp,i} \delta_{jk} + 2\mu S_{jk,i}) l^2 + (f_1 \delta_{jk} P_i + f_2 \delta_{ij} P_k + f_2 \delta_{ik} P_j) \quad (24)$$

$$E_i = a P_i + f_1 S_{kk,i} + 2f_2 S_{ij,j} \quad (25)$$

Substituting the relations above into the governing equations (4) and (2) and making use of Eq. (1), we get

$$\nabla^2 (a \varepsilon \varphi + f u_{k,k}) = 0 \quad (26)$$

$$(\lambda + \mu)(1 - l_1^2 \nabla^2) u_{k,kj} + \mu(1 - l_2^2 \nabla^2) u_{j,kk} = 0 \quad (27)$$

where $f = f_1 + 2f_2$, $\nabla^2 = \partial_{ii}$ is the Laplacian operator and l_1, l_2 are some material length scales given by

$$l_1^2 = l^2 - \frac{\varepsilon_0 f^2}{(\lambda + \mu) a \varepsilon} + \frac{f_2^2}{(\lambda + \mu) a}, \quad l_2^2 = l^2 - \frac{f_2^2}{a \mu} \quad (28)$$

Note that Eq. (27) differs from that of Aravas [48] in that we have two length scales l_1 and l_2 while he has only l . We observe from Eq. (28) that this is due to the flexoelectric effect. Interestingly, the form of Eq. (27) is the same as the Navier equation of general strain-gradient elasticity proposed by Mindlin [38], but his length scales have nothing to do with electromechanical coupling. However, Mindlin's argument concerning the positive definiteness of the energy [38] still applies here. Thus, l_1 and l_2 have to be real in order to guarantee positive definiteness of the strain energy and preserve the uniqueness of the solution to the Navier equations. This imposes a limit on flexoelectric constants.

5 Solutions to Boundary Value Problems

5.1 Beam Bending. Consider a slender beam on the $\mathbf{e}_1 - \mathbf{e}_2$ plane, with length L and thickness $2h$ (with width b). The coordinate x_1 runs along the length of the beam through the centroid of the cross section and x_2 lies along the thickness of the beam. We assume $L \gg 2h$, so that gradients in the \mathbf{e}_2 direction are much larger than the gradients in the \mathbf{e}_1 direction. We will work out the leading order solution to our beam problems based on Euler–Bernoulli theory, which postulates

$$S_{11} = -\kappa x_2, \quad S_{22} = \kappa l x_2, \quad S_{12} = 0 \quad (29)$$

where κ is the curvature. The stresses are

$$T_{11} = -E \kappa x_2, \quad T_{22} = T_{12} = 0 \quad (30)$$

where E is the Young's modulus. In addition, suppose that the left end and right end of the beam are open ($D_1 = 0$) and a potential is applied between upper surface where $\varphi(x_1, h) = V$, and lower surface where $\varphi(x_1, -h) = 0$. The leading order solution of Eq. (26) is

$$\varphi = \frac{V}{2} \left(1 + \frac{x_2}{h} \right) = \beta x_2 + \frac{V}{2} \quad (31)$$

where $\beta = V/2h$. Using the above we see that

$$P_2 = (\varepsilon - \varepsilon_0)(f_b \kappa - \beta), \quad D_2 = -\varepsilon_0 \beta + P_2, \quad \hat{T}_{211} = E l^2 \kappa + f_1 P_2, \quad \hat{T}_{112} = f_2 P_2, \quad \hat{T}_{222} = f P_2 \quad (32)$$

where $f_b = f_1 - \nu f$ is the effective flexoelectric constant in beam bending. This result has been widely used in measurements of flexoelectric constants that utilize a beam system [14–16]. Now, using the above equations we can rewrite the stored energy density W as a function of κ and D_2

$$W(\kappa, D_2) = \frac{1}{2} (x_2^2 + l^2 - l_f^2 / (a \varepsilon)) E \kappa^2 + \frac{1}{2} \varepsilon^{-1} D_2^2 - f_b D_2 \kappa / (a \varepsilon) \quad (33)$$

where $l_f = \sqrt{\varepsilon_0 f_b^2 / E}$ is a flexoelectric length scale. l_f / l is a measure of the importance of flexoelectricity compared to SGE. By integrating along the thickness direction x_2 , the total energy of the beam can be written as

$$\int_V W dv = \int_0^L \frac{1}{2} \left(G_D \kappa^2 - 2 \frac{f_b D_2 \kappa}{a \varepsilon} + \frac{D_2^2}{\varepsilon} \right) dx_1 = \int_0^L W_b dx_1 \quad (34)$$

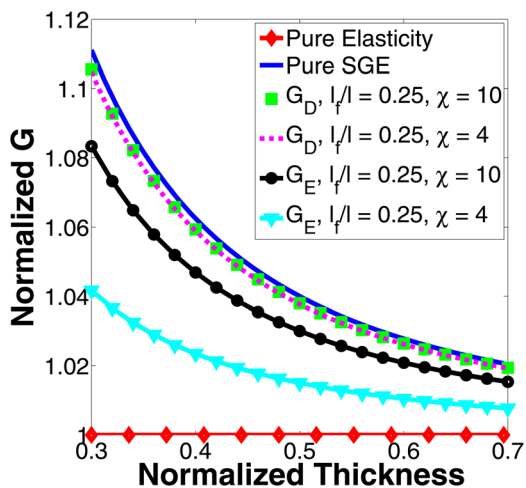


Fig. 1 Size-dependent stiffening of flexoelectric beams. χ in the legend is the susceptibility constant. The bending rigidity plotted on the y -axis is normalized against EI where E is the Young's modulus and I is the moment of inertia of the cross section. The thickness of the beam is normalized against $\sqrt{3I}$. As the beam gets thinner the strain gradients increase, so the effects of flexoelectricity become more prominent.

where $G_D = E[I + Al^2 - Al_f^2/(a\epsilon)]$ with A denoting the cross sectional area and I the moment of inertia. The principle of virtual work yields the relation

$$\frac{\partial W_b}{\partial \kappa} = M(x_1) = G_D \kappa - \frac{f_b}{a\epsilon} D_2 = G_E \kappa + a^{-1} f_b \beta A \quad (35)$$

where M is the bending moment and $G_E = E[I + Al^2 - Al_f^2/(a\epsilon_0)]$. Note that the bending rigidity of the beam is G_E when $\beta = (V/2h) = 0$ or the electric field is zero, while it is G_D when the electric displacement $D_2 = 0$. Note also that $G_D > G_E$ because $\epsilon > \epsilon_0$ and the enhancement is proportional to f_f^2 or f_b^2 . A similar effect is also observed in beams made of piezoelectric materials [51]. But, in contrast to piezoelectric beams, the stiffening in flexoelectric beams is highly size-dependent as shown in Fig. 1.

Euler–Bernoulli beam theory requires

$$M'' = G_D \kappa'' - \frac{f_b}{a\epsilon} D_2'' = q(x_1), \quad Q = -M' \quad (36)$$

where M' denotes (dM/dx_1) , $q(x_1)$ is the distributed load and Q is the shear force. The equation above and our prediction of a size-dependent bending rigidity which is enhanced proportionally to f_b^2 , agree with the results of Refs. [22,23,34]. Recognizing that $\kappa = (d^2 u_2/dx_1^2)$, we can easily integrate the above equation for given loading and boundary conditions to get the deflection profile of the neutral axis of the beam $u_2(x_1)$.

The solutions of the equation above can be used to measure flexoelectric constants. However, as pointed out in Ref. [20], this can only give us f_b . We are not able to determine all the flexoelectric constants even for simple cubic crystals. One can try to

measure the horizontal polarization P_1 to get some more information, but this is difficult since the average P_1 in any cross section vanishes. This happens because the corresponding strain gradient $S_{11,1}$ is linear in y . This difficulty, however, can be overcome by use of a horizontal loading which shifts the neutral axis of the beam away from its centroid by some amount d . Assuming that this does not perturb the bending solution by much we can calculate the average horizontal polarization as

$$P_1^{avg} = \frac{1}{2h} \int_{-h+d}^{h+d} \frac{1-\nu}{a} f \kappa' y dy \approx \frac{1-\nu}{a} f \kappa' d \quad (37)$$

given that d/h is not too large. A precise measurement of this smaller quantity will give us another equation to completely determine the flexoelectric constants in an isotropic material and help determine that of cubic crystals.

5.2 Example of Reciprocity.

We will use our solution to the flexoelectric beam to demonstrate the reciprocal theorem. Consider two problems (see Fig. 2) for two clamped–clamped beams with exactly same geometries (thickness $2h$, width b , and length L). In the original problem, a force Q is exerted at $x_1 = L_1$; in the reciprocal problem, a constant voltage V is prescribed across the beam from L_2 to L . We model this voltage as a step function and neglect edge effects. The deflection profile of the beam is $u_2(x_1)$. The variables in the original problem will have upper index 1 and those in the reciprocal problem will have upper index 2.

We will start with the reciprocal problem. Since there is no distributed load along the beam, Eqs. (36) and (35) give

$$\kappa^{(2)} = \frac{d^2 u_2^{(2)}}{dx_1^2} = -\frac{f_b A}{a G_E} \beta H(x_1 - L_2) = -\frac{\beta}{V_b} H(x_1 - L_2) \quad (38)$$

where V_b is introduced to avoid redundant repetition of constants and H is the unit step function. We will use the Macaulay bracket $\langle \rangle^n$ to denote the n th antiderivative of H . By applying the clamped boundary conditions at the two ends, the deflection profile in the reciprocal problem can be calculated

$$u_2^{(2)}(x_1) = \frac{\beta}{V_b} \left[-\frac{1}{2} \langle x_1 - L_2 \rangle^2 + L_2(L - L_2) \frac{x_1^3}{L^3} + (L - L_2)(L - 3L_2) \frac{x_1^2}{2L^2} \right] \quad (39)$$

Using this, we are able to determine $\mathcal{W}^{(12)}$

$$\begin{aligned} \mathcal{W}^{(12)} &= Q u_2^{(2)}(L_1) \\ &= \frac{QV}{4hV_b} \left[-\langle L_1 - L_2 \rangle^2 + 2L_2(L - L_2) \frac{L_1^3}{L^3} + (L - L_2)(L - 3L_2) \frac{L_1^2}{L^2} \right] \end{aligned} \quad (40)$$

For the original problem, the deflection and electric displacement are given by

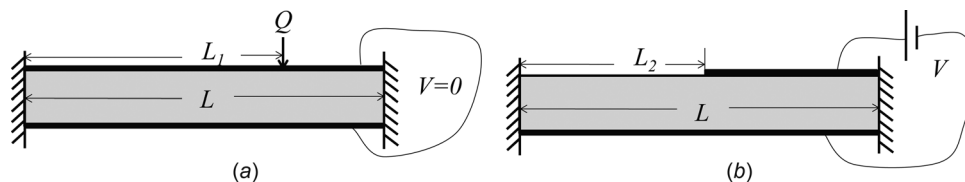


Fig. 2 In (a), a point load Q is applied, while in (b) there is a potential difference between the upper and lower surface over a portion of the beam

$$u_2^{(1)}(x_1) = \frac{Q}{6G_E} \left[- (L - L_1)^2(L + 2L_1) \frac{x_1^3}{L^3} + 3(L - L_1)^2 L_1 \frac{x_1^2}{L^2} + \langle x_1 - L_1 \rangle^3 \right] \quad (41)$$

$$D_2^{(1)}(x_1) = \frac{f_b}{a} \kappa^{(1)} = \frac{Q}{AV_b} \left[- (L - L_1)^2(L + 2L_1) \frac{x_1}{L^3} + \frac{(L - L_1)^2 L_1}{L^2} + \langle x_1 - L_1 \rangle \right] \quad (42)$$

Hence, we are able to calculate $\mathcal{W}^{(21)}$ as

$$\begin{aligned} \mathcal{W}^{(21)} &= -b \int_{L_2}^L D_2^{(1)} V dx_1 \\ &= \frac{QV}{4hV_b} \left[\frac{L_2(L - L_1)^2}{L^3} (2L_1L - 2L_2L_1 - LL_2) + \langle L_2 - L_1 \rangle^2 \right] \end{aligned} \quad (43)$$

Note that $\langle L_1 - L_2 \rangle^2 + \langle L_2 - L_1 \rangle^2 = (L_1 - L_2)^2$, so $\mathcal{W}^{(12)} = \mathcal{W}^{(21)}$.

5.3 Torsion. Torsion of circular shafts generates a constant strain gradient. Surprisingly, such a strain gradient does not polarize an isotropic flexoelectric material. To see why, let us start with the displacement field of a circular shaft under torsion with e_3 aligned with the axis of the shaft

$$u_1 = -\phi x_2 x_3, \quad u_2 = \phi x_1 x_3, \quad u_3 = 0 \quad (44)$$

where ϕ is the angle of twist per unit length. The strains are

$$S_{13} = -\frac{1}{2} \phi x_2, \quad S_{23} = \frac{1}{2} \phi x_1 \quad (45)$$

The nonvanishing components of the strain gradient are $S_{13,2}$, $S_{31,2}$ and $S_{23,1}$, $S_{32,1}$. By use of Eq. (22), the flexoelectric contribution to the energy is

$$W_f = f_1 S_{kk,i} P_i + 2f_2 S_{ij,i} P_j = 0 \quad (46)$$

no matter which direction polarization takes. As a result, a circular shaft made of isotropic flexoelectric material will not polarize under torsion even though strain-gradient effects will lead to a size-dependent torsional rigidity. This result also holds for cubic crystals, where the flexoelectric tensor takes the following form [52]:

$$f_{ijkl} = f_1 \delta_{jk} \delta_{il} + f_2 (\delta_{ij} \delta_{kl} + \delta_{ik} \delta_{jl}) + f_3 \delta_{ijkl} \quad (47)$$

where f_3 is another flexoelectric constant and δ_{ijkl} is the fourth-order Kronecker Delta which is 1 when i, j, k, l are all equal and 0 otherwise. If the axis of the shaft is aligned with one of the sides of the cubic lattice, then the flexoelectric contribution to the energy is

$$W_f = f_1 S_{kk,i} P_i + 2f_2 S_{ij,i} P_j + f_3 S_{ii,i} P_i = 0 \quad (48)$$

which vanishes.

5.4 Disk Under Pressure. Calculating the stress in a circular disk or cylinder with a central hole under internal and/or external pressure is a classic problem in linear elasticity, just as calculating

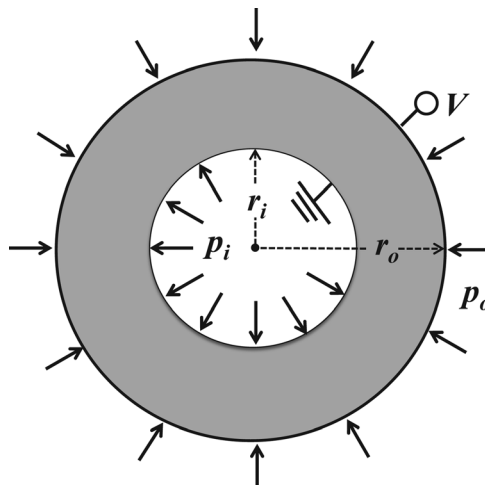


Fig. 3 A disk/cylinder, with inner and outer radius r_i and r_o . It is subject to a potential difference V_0 between the surfaces as well as internal and external pressure p_i and p_o .

the capacitance of a cylindrical capacitor is in electrostatics. The solution in this simple geometry offers not only a direct comparison to classical elasticity and SGE but also some insights into the stress and polarization fields near point defects in flexoelectric materials. The geometry of the problem is illustrated in Fig. 3. It is convenient to solve this axisymmetric problem in polar coordinates so that the only relevant component of displacement is $u_r = u(r)$. Hence, the Navier equation (27) can be simplified to

$$\left(1 - l_0^2 \nabla^2 + \frac{l_0^2}{r^2} \right) \left(\nabla^2 u(r) - \frac{u(r)}{r^2} \right) = 0, \quad l_0^2 = l^2 - \frac{(1 - \nu^2) l_f^2}{a \varepsilon} \quad (49)$$

where $l_f = \sqrt{\varepsilon_0 f^2 / E}$ is the flexoelectric length scale in this problem. From here on, we will avoid the use of a as a material constant and work with ε and ε_0 . The general solution to this equation is of the form [48,53]

$$u(r) = ar + \frac{b}{r} + cI_1(\lambda_0 r) + dK_1(\lambda_0 r) \quad (50)$$

where $\lambda_0 = l_0^{-1}$ and a, b, c, d are constants to be determined by BCs, I_i and K_i denote i th order modified Bessel function of the first and second kind respectively. Once we have the displacement field, the solution to the potential $\varphi = \varphi(r)$ can be readily worked out using

$$\nabla^2 \varphi = -\frac{(\varepsilon - \varepsilon_0) f}{\varepsilon} \nabla^2 \left(u_r + \frac{u}{r} \right) \quad (51)$$

whose general solution is given by

$$\varphi = -\frac{(\varepsilon - \varepsilon_0) f}{\varepsilon} [2a + c\lambda_0 I_0(\lambda_0 r) - d\lambda_0 K_0(\lambda_0 r)] + g + h \ln r \quad (52)$$

where g and h are constants to be obtained from BCs. We have six unknown constants, hence six BCs are needed to solve for them. From Fig. 3, we can see that traction and potential are specified at both inner and outer surfaces. Only two other BCs are needed and they are related to the higher-order stresses \hat{T}_{ijk} which depend on the polarization field whose only nonzero component is

$$P_r = -(\varepsilon - \varepsilon_0) [\varphi_{,r} + f(u_{,rr} + r^{-1} u_{,r})] \quad (53)$$

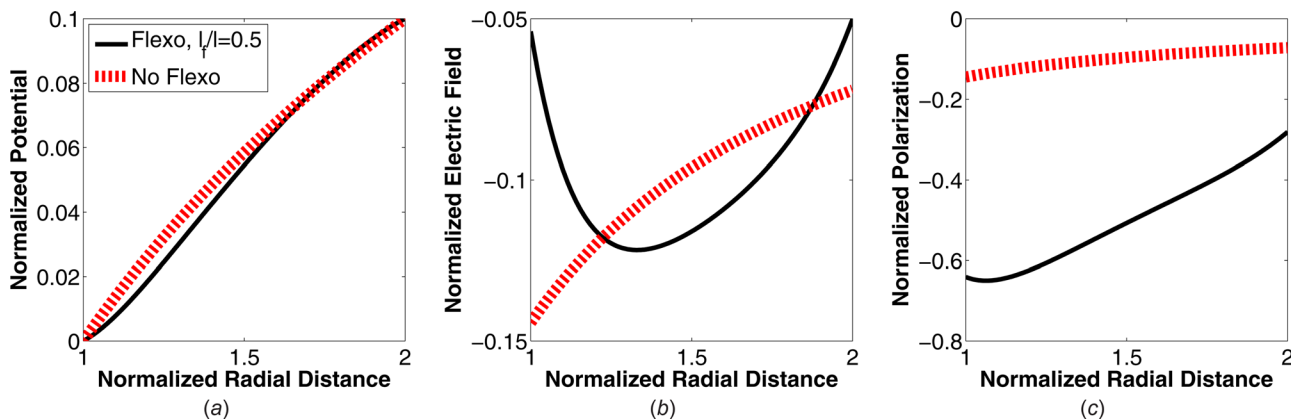


Fig. 4 Variation of the electric quantities along the radial direction in the disk loaded by internal/external pressure. We choose $r_o/r_i = 2$, $p_o/p_i = 2$, $\nu = 0.3$, $\chi = 1$, $l = 0.2r_i$, and $l_f = 0.5l$, as in the legend. All quantities are normalized to be nondimensional, in the unit system where length, force, and charge are measured by r_i , $E r_i^2$, and $r_i^2 \sqrt{\epsilon_0 E}$ respectively.

The expressions for the nonzero components of \hat{T}_{ijk} are given below:

$$\begin{aligned} \hat{T}_{rrr} &= l^2 \frac{\partial T_{rr}}{\partial r} + f P_r, & \hat{T}_{r\theta\theta} &= l^2 \frac{\partial T_{\theta\theta}}{\partial r} + f_1 P_r, \\ \hat{T}_{\theta r\theta} &= \hat{T}_{\theta\theta r} = l^2 \frac{T_{rr} - T_{\theta\theta}}{r} + f_2 P_r \end{aligned} \quad (54)$$

Thus, the higher-order traction \hat{p} on the outer boundary is

$$\hat{p}(r) = \hat{T}_{rrr} = l^2 \frac{\partial T_{rr}}{\partial r} + f P_r \quad (55)$$

The pressure on the outer boundary is

$$\begin{aligned} p(r) &= T_{rr} - \hat{T}_{rrr,r} + \frac{2\hat{T}_{\theta r\theta} + \hat{T}_{r\theta\theta}}{r} \\ &= \left(1 + 2\frac{l^2}{r^2} - l^2 \frac{\partial^2}{\partial r^2}\right) T_{rr} + \left(-2\frac{l^2}{r^2} + \frac{l^2}{r} \frac{\partial}{\partial r}\right) T_{\theta\theta} + \frac{f P_r}{r} \end{aligned} \quad (56)$$

Finally, the six boundary conditions required to determine the six constants in our solution are

$$\begin{aligned} p(r_o) &= -p_o, & p(r_i) &= -p_i; & \hat{p}(r_o) &= \hat{p}(r_i) = 0; \\ \varphi(r_o) &= V_o, & \varphi(r_i) &= 0 \end{aligned} \quad (57)$$

We can solve for these constants, but the expressions are lengthy and un insightful. Instead, we plot the results for the polarization, stress, and displacement fields for a specific geometry with $(r_o/r_i) = 2$ in order to garner some insights. We fix the strain gradient and flexoelectric length scales so that $(l/r_i) = 0.2$ and $(l_f/l) = 0.5$. The electric quantities are plotted in Figs. 4(a)–4(c). The potential, electric field, and polarization in the absence of flexoelectricity are shown as dashed lines while those with flexoelectricity are shown as solid lines. The polarization and electric field are significantly perturbed by the flexoelectric effect. The displacement and strain fields are plotted in Fig. 5. Due to the flexoelectric effect, the displacement is significantly reduced compared to the classical elasticity solution and the SGE solution (see Fig. 5(a)). The hoop strain $\epsilon_{\theta\theta}$ is also significantly reduced (see Fig. 5(c)) and the variation of radial strain ϵ_{rr} is smoothed out due to the flexoelectric effect (see Fig. 5(b)). Smaller strains imply higher rigidity of the disk. This is reminiscent of the increased rigidity we saw earlier in the flexoelectric beam.

Next we would like to plot the stresses. This presents a problem because the Cauchy stress of classical elasticity no longer represents the “true” physical stress in materials with SG effects. However, according to Refs. [38,48], the true stress σ_{ij} can still be computed through the following equation:

$$\sigma_{ij} = T_{ij} - \frac{2}{3} \hat{T}_{ijk,k} - \frac{1}{3} \hat{T}_{kij,k} \quad (58)$$

A direct result of the above equation is that σ_{ij} (referred to as stress afterwards) is no longer symmetric. In general, σ_{ij} and T_{ij}

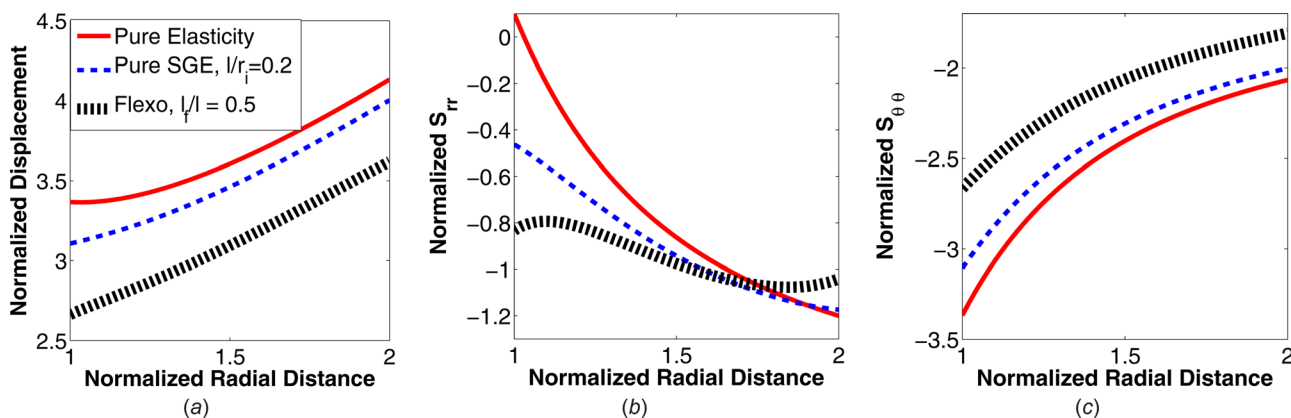


Fig. 5 Variation of displacement and strains in the disk loaded by internal/external pressure. (a) Normalized magnitude of displacement. (b) and (c) plot the radial and circumferential normal strain respectively.

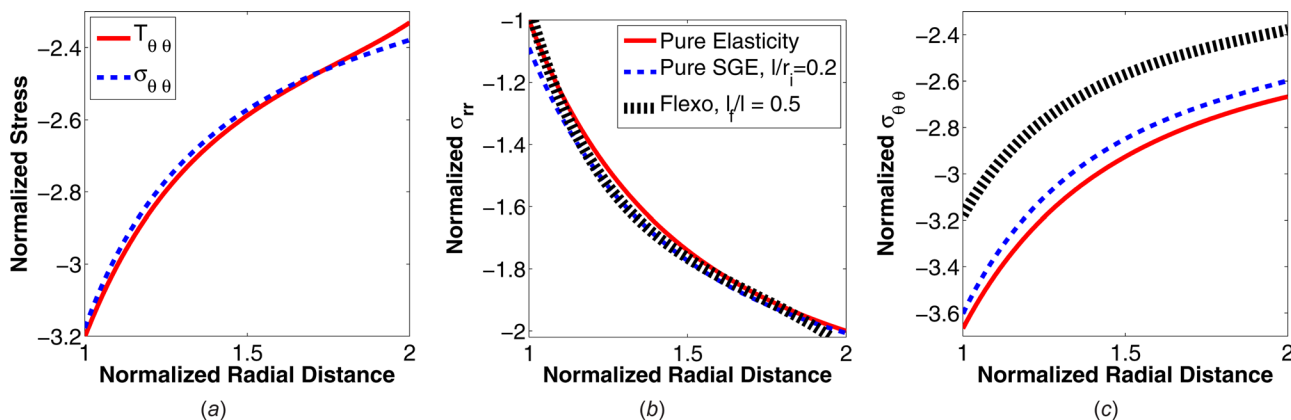


Fig. 6 Stresses in the disk loaded by internal/external pressure. (a) Compares the profiles of the $\theta\theta$ component of the true stress and Cauchy stress, they differ by little. (b) and (c) plot the radial and circumferential normal true stress respectively.

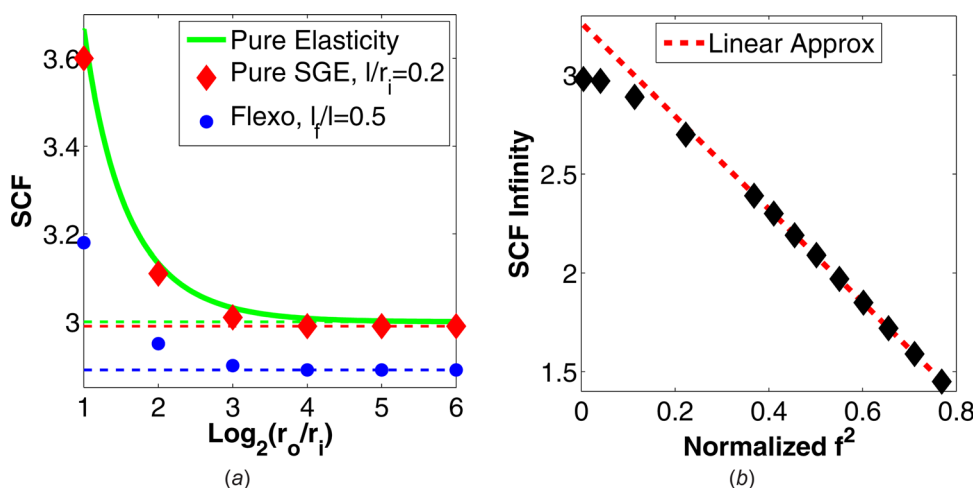


Fig. 7 Stress concentration factor in the disk loaded by internal/external pressure. (a) plots the asymptotic behavior of SCF with $r_o/r_i \rightarrow \infty$. (b) plots the flexoelectric reduction of SCF^∞ with increasing f . f^2 is normalized against f_{max}^2 whose value is determined by requiring the energy to be positive definite.

can be very different, but there are cases where Cauchy stress is a good approximation of the true stress. This happens to be true for this problem as shown in Fig. 6(a). The other components of the true stress are also plotted in Fig. 6. From Figs. 6(b) and 6(c), it is clear that hoop stress is larger than the radial stress and is also significantly altered by the flexoelectric effect. Accordingly, we define a SCF as follows:

$$SCF = \frac{|\sigma_{\theta\theta}|_{max}}{p_i} = -\frac{\sigma_{\theta\theta}}{p_i} \Big|_{r=r_i} \quad (59)$$

From Fig. 6(c), it is apparent that flexoelectricity reduces the SCF compared to classical elasticity or SGE. This happens because in a flexoelectric material, part of the work done by the external loads is used to polarize the material. This is in contrast to elasticity where all the work done by the external loads is stored as elastic energy in the body.

In Fig. 7(a), we plot SCF as a function of r_o/r_i while keeping $l/l = 0.5$. We also plot SCF for the pure elasticity and SGE solutions. As $r_o/r_i \rightarrow \infty$, $SCF \rightarrow SCF^\infty$, a constant. For the flexoelectric solid, $SCF_{Flex}^\infty = 2.89 < SCF_{SGE}^\infty = 2.99 < SCF_{Elast}^\infty = 3.00$. Note that if f is larger than more of the external mechanical work will be converted into electrical energy. With this in mind, we calculate SCF^∞ as a function of f in Fig. 7(b). As $f \rightarrow 0$, we recover

$SCF_{SGE}^\infty = 2.99$ and when f approaches the limit f_{max} (dictated by positive definiteness of the energy), SCF^∞ reduces sharply (approximately proportional to f^2). Figure 7(b) shows that at $f = 0.9f_{max}$, SCF^∞ is reduced by more than 50%. Even in cases where f is not as large, it is possible to alter SCF by applying a stronger potential difference V_0 between the inner and outer surfaces of the disk. This is shown in Fig. 8(a). A linear reduction of SCF is observed as the potential V_0 is increased. This reduction becomes more and more sensitive to V_0 as f becomes larger. From another perspective, this result implies that it is possible to modulate material strength through external electric fields. In fact, this modulation is proportional to the magnitude of external field and becomes stronger in materials with larger flexoelectric constants. Similarly, the electrical behavior can be controlled by changing the mechanical loading. Figure 8(b) shows that the magnitude of polarization (at r_i) increases proportionally with p_i while $V_0 = 0$ is held fixed. This is a straightforward result of the dominating SG induced polarization.

In order to see any of these effects in experiments, it is important to get some estimates of f_{max} . Note that

$$f_{max} \approx \sqrt{\frac{E}{\epsilon_0(1-\nu^2)}} l \sim l \times 10^{10} V \quad (60)$$

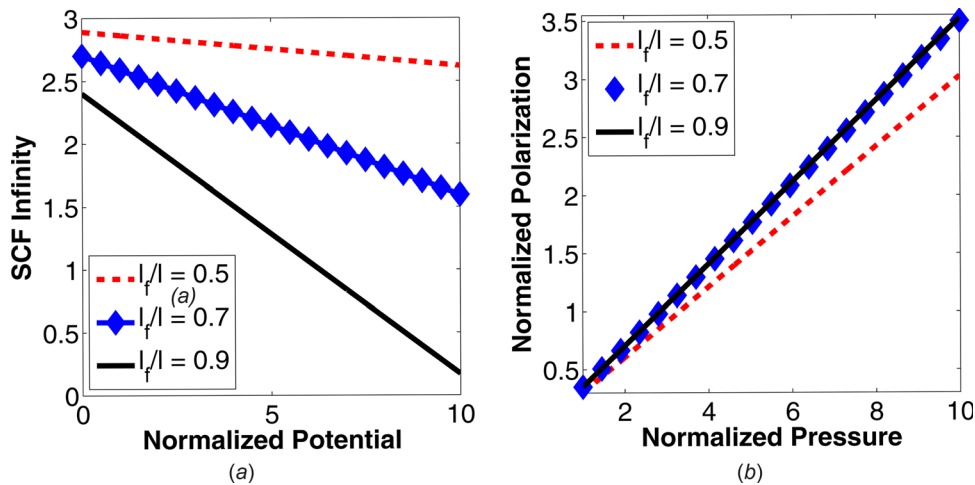


Fig. 8 Modulation of mechanical/electrical quantities in disk loaded by internal/external pressure. (a) plots SCF^∞ as a function of potential V_o holding p_o and p_i fixed. (b) plots polarization at the inner surface as a function of pressure p_i , holding $V_o = 0$. Nondimensionalization is carried out in the same manner as in Fig. 4.

Thus, the magnitude of f_{max} is closely related to SGE length scale. As suggested in Ref. [54], l is on the order of several to tens of nm while the classical estimate for f is $f \sim 1-10$ V for simple ionic crystals [12]. This is consistent with our estimate in Eq. (60) above. However, f for simple ionic crystals (such as, sodium chloride) is so small [28] that it is difficult to perform reliable measurements. In contrast, experimental measurements carried out on perovskite materials, e.g. barium titanate, are relatively well documented. These materials exhibit an f that is several orders of magnitude greater than that of simple ionic crystals like sodium chloride [20]. Thus, our predicted flexoelectric reduction of SCF and its interplay with elasticity should be observable in these materials. For these reasons, perovskite materials are now at the cutting edge of the research on flexoelectricity.

We note here that the study of SGE and flexoelectricity are tightly connected. As in SGE our discussion of flexoelectricity is valid only when r_i is comparable to l . In other words, this effect is important only at nanometer length scales. If the inner diameter of the disk is on the order of cm, it can be shown that the solution we obtained converges to that of classical elasticity. Hence, our prediction of an electric field dependent enhancement of strength applies only to nanometer scale specimens of flexoelectric solids.

5.5 In-Plane Shear of a Disk. It is also possible to solve a BVP for a disk under in-plane shear. The only surviving term of displacement here is $u_\theta = v(r)$. As a result, the Navier equation for this problem is of the same type as the previous one

$$\left(1 - l_2^2 \nabla^2 + \frac{l_2^2}{r^2}\right) \left(\nabla^2 v(r) - \frac{v(r)}{r^2}\right) = 0 \quad (61)$$

In this problem $l_f^2 = l^2 - l_2^2 = (\epsilon - \epsilon_0) f_2^2 / \mu$, and the general solution of Eq. (61) is again given by

$$v(r) = ar + \frac{b}{r} + cI_1(\lambda_2 r) + dK_1(\lambda_2 r) \quad (62)$$

where $\lambda_2 = l_2^{-1}$ and a, b, c, d are some constants to be determined by BCs. We employ the same method as above to solve the problem with the following boundary conditions:

$$v(r_i) = 0, \tau(r_o) = \tau_0; \quad \hat{\tau}(r_i) = \hat{\tau}(r_o) = 0; \quad \varphi(r_i) = \varphi(r_o) = 0 \quad (63)$$

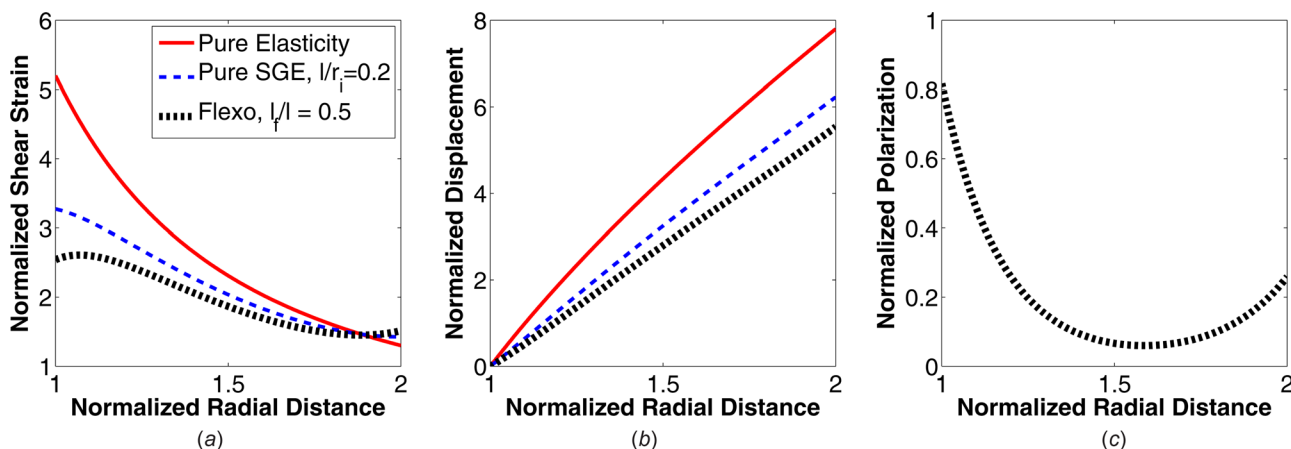


Fig. 9 A solution for the in-plane shear of a disk is obtained with the following parameters: $r_o/r_i = 2$, $\tau_0/E = 1$, $\nu = 0.3$, $\chi = 1$, $l = 0.2r_i$, and $l_f = 0.5l$. (a) plots normalized shear strain and (b) the normalized displacement as functions of the radial coordinate. (c) plots the distribution of normalized azimuthal polarization. It reaches a minimum around the middle of the disk. Note that all quantities are nondimensionalized, in the same manner as in Fig. 4.

Here, τ and $\hat{\tau}$ denote the usual and higher-order traction respectively. This type of BCs correspond to a disk being sheared from outside with inside held fixed. The last two BCs tell us that there is no potential difference applied between the outer and inner surface of the disk. We plot the displacement, strain, and polarization fields for a specific choice of parameters in Fig. 9. The results confirm the features observed in earlier results: (a) smaller displacements for the same boundary loads, (b) smoother strain profiles compared to pure elasticity or strain-gradient elasticity, and (c) increase in rigidity. We attribute these features to flexoelectricity.

Interestingly, in this problem, the displacement field is divergence-free. As a result the governing equation for φ is completely decoupled from the deformation. However, the inhomogeneous strain field produces an azimuthal polarization P_θ

$$P_\theta = -\frac{(\varepsilon - \varepsilon_0)f_2}{2l_2^2}[cI_1(\lambda_2 r) + dK_1(\lambda_2 r)] \quad (64)$$

The magnitude of the azimuthal polarization shows an interesting variation—it is maximum at the boundaries and smaller inside. Note that the polarization is completely determined by c and d and it is only observable at length scales comparable to l . A piezoelectric problem with the same geometry and loading gives a radial polarization. The azimuthal polarization predicted here for a disk made of flexoelectric material can potentially be verified by experiments.

6 Conclusions

In this paper, we have formulated the governing equations for a flexoelectric solid and a Navier equation for isotropic flexoelectric material, under the assumptions of small strains. We have used a linear constitutive law and proved a reciprocal theorem for flexoelectricity. An analogous theorem for piezoelectric materials is well known. We have used our theory to solve some boundary value problems for isotropic flexoelectric materials. While there are many known analytic solutions to boundary value problems for piezoelectric solids there are few, if any, known solutions for flexoelectric solids. Our solutions could be useful in the interpretation of nanoscale experiments in the burgeoning field of flexoelectric materials. They also indicate how the mechanical behavior of a flexoelectric material can be modulated at the nanoscale by the use of electric fields. The methods discussed in this paper could be a starting point for building continuum-based computational methods for flexo-electric solids. Such methods will be required to compute displacement and polarization fields in complex geometries where analytical solutions are not possible.

Acknowledgment

We acknowledge support for this work through the Army Research Office Grant No. W911NF-11-1-0494. We thank Mr. Jian Han and Professor David Srolovitz for insightful discussions.

References

- [1] Landau, L. D., Lifshitz, E. M., and Pitaevskii, L., 1984, *Electrodynamics of Continuous Media*, Pergamon Press, UK.
- [2] Maugin, G. A., and Eringen, A. C., 1990, *Electrodynamics of Continua*, Springer-Verlag, Berlin.
- [3] Kovetz, A., 2000, *Electromagnetic Theory*, Oxford, New York.
- [4] Meyer, R. B., 1969, "Piezoelectric Effects in Liquid Crystals," *Phys. Rev. Lett.*, **22**(18), pp. 918–921.
- [5] Buka, A., and Eber, N., 2012, *Flexoelectricity in Liquid Crystals: Theory, Experiments and Applications*, Imperial College Press, London.
- [6] Raphael, R. M., Popel, A. S., and Brownell, W. E., 2010, "A Membrane Bending Model of Outer Hair Cell Electromotility," *Biophys. J.*, **78**(6), pp. 2844–2862.
- [7] Petrov, A. G., 2006, "Electricity and Mechanics of Biomembrane Systems: Flexoelectricity in Living Membranes," *Anal. Chim. Acta*, **568**(1–2), pp. 70–83.

- [8] Petrov, A. G., 2002, "Flexoelectricity of Model and Living Membranes," *Biochim. Biophys. Acta*, **1561**(1), pp. 1–25.
- [9] Harland, B., Brownell, W. E., Spector, A. A., and Sun, S. X., 2010, "Voltage-Induced Bending and Electromechanical Coupling in Lipid Bilayers," *Phys. Rev. E*, **81**(3), p. 031907.
- [10] Mashkevich, V. S., and Tolpygo, K. B., 1957, "Electrical, Optical and Elastic Properties of Diamond Type Crystals. I," *Sov. Phys. JETP*, **5**, pp. 435–439.
- [11] Tolpygo, K. B., 1963, "Long Wavelength Oscillations of Diamond-Type Crystals Including Long Range Forces," *Sov. Phys. Sol. State*, **4**, pp. 1297–1305.
- [12] Kogan, S. M., 1964, "Piezoelectric Effect During Inhomogeneous Deformation and Acoustic Scattering of Carriers in Crystals," *Sov. Phys. Sol. State*, **5**, pp. 2069–2070.
- [13] Tagantsev, A. K., 1991, "Electric Polarization in Crystals and Its Response to Thermal and Elastic Perturbations," *Phase Transitions*, **35**(3–4), pp. 119–203.
- [14] Ma, W., and Cross, L. E., 2001, "Large Flexoelectric Polarization in Ceramic Lead Magnesium Niobate," *Appl. Phys. Lett.*, **79**(26), pp. 4420–4422.
- [15] Ma, W., and Cross, L. E., 2002, "Flexoelectric Polarization of Barium Strontium Titanate in the Paraelectric State," *Appl. Phys. Lett.*, **81**(18), pp. 3440–3442.
- [16] Zubko, P., Catalan, G., Buckley, A., Welche, P. R. L., and Scott, J. F., 2007, "Strain-Gradient-Induced Polarization in SrTiO₃ Single Crystals," *Phys. Rev. Lett.*, **99**(16), p. 167601.
- [17] Eliseev, E. A., Morozovska, A. N., Glinchuk, M. D., and Blinc, R., 2009, "Spontaneous Flexoelectric/Flexomagnetic Effect in Nanoferroelectrics," *Phys. Rev. B*, **79**(16), p. 165433.
- [18] Lee, D., Yoon, A., Jang, S. Y., Yoon, J.-G., Chung, J.-S., Kim, M., Scott, J. F., and Noh, T. W., 2011, "Giant Flexoelectric Effect in Ferroelectric Epitaxial Thin Films," *Phys. Rev. Lett.*, **107**(5), p. 057602.
- [19] Nguyen, T. D., Deshmukh, N., Nagaraj, J. M., Kramer, T., Purohit, P. K., Berry, M. J., and McAlpine, M. C., 2012, "Piezoelectric Nanoribbons for Monitoring Cellular Deformations," *Nat. Nanotechnol.*, **7**(9), pp. 587–593.
- [20] Zubko, P., Catalan, G., and Tagantsev, A. K., 2013, "Flexoelectric Effect in Solids," *Annu. Rev. Mater. Res.*, **43**(1), pp. 387–421.
- [21] Catalan, G., Lubk, A., Vlooswijk, A. H. G., Snoeck, E., Magen, C., Janssens, A., Rispens, G., Rijnders, G., Blank, D. H. A., and Noheda, B., 2011, "Flexoelectric Rotation of Polarization in Ferroelectric Thin Films," *Nat. Mater.*, **10**(12), pp. 963–967.
- [22] Majdoub, M. S., Sharma, P., and Cagin, T., 2008, "Enhanced Size-Dependent Piezoelectricity and Elasticity in Nanostructures Due to the Flexoelectric Effect," *Phys. Rev. B*, **77**(12), p. 125424.
- [23] Majdoub, M. S., Sharma, P., and Çağın, T., 2009, "Erratum: Enhanced Size-Dependent Piezoelectricity and Elasticity in Nanostructures Due to the Flexoelectric Effect," *Phys. Rev. B*, **79**(11), p. 119904.
- [24] Sharma, N. D., Landis, C. M., and Sharma, P., 2010, "Piezoelectric Thin-Film Superlattices Without Using Piezoelectric Materials," *J. Appl. Phys.*, **108**(2), p. 024304.
- [25] Sharma, N. D., Landis, C., and Sharma, P., 2012, "Erratum: Piezoelectric Thin-Film Super-Lattices Without Using Piezoelectric Materials," *J. Appl. Phys.*, **111**(5), p. 059901.
- [26] Ahluwalia, R., and Srolovitz, D., 2007, "Size Effects in Ferroelectric Thin Films: 180° Domains and Polarization Relaxation," *Phys. Rev. B*, **76**(17), p. 174121.
- [27] Tagantsev, A. K., 1985, "Theory of Flexoelectric Effect in Crystals," *Zh. Eksp. Teor. Fiz.*, **88**, pp. 2108–2122.
- [28] Maranganti, R., and Sharma, P., 2009, "Atomistic Determination of Flexoelectric Properties of Crystalline Dielectrics," *Phys. Rev. B*, **80**(5), p. 054109.
- [29] Kalinin, S. V., and Meunier, V., 2008, "Electronic Flexoelectricity in Low-Dimensional Systems," *Phys. Rev. B*, **77**(3), p. 033403.
- [30] Resta, R., 2010, "Towards a Bulk Theory of Flexoelectricity," *Phys. Rev. Lett.*, **105**(12), p. 127601.
- [31] Hong, J., and Vanderbilt, D., 2011, "First-Principles Theory of Frozen-Ion Flexoelectricity," *Phys. Rev. B*, **84**(18), p. 180101.
- [32] Hong, J., Catalan, G., Scott, J. F., and Artacho, E., 2010, "The Flexoelectricity of Barium and Strontium Titanates From First Principles," *J. Phys.: Condens. Matter*, **22**(11), p. 112201.
- [33] Nguyen, T. D., Mao, S., Yeh, Y.-W., Purohit, P. K., and McAlpine, M. C., 2013, "Nanoscale Flexoelectricity," *Adv. Mater.*, **25**(7), pp. 946–974.
- [34] Yan, Z., and Jiang, L. Y., 2013, "Flexoelectric Effect on the Electroelastic Responses of Bending Piezoelectric Nanobeams," *J. Appl. Phys.*, **113**(19), p. 194102.
- [35] Suo, Z., Zhao, X., and Greene, W., 2008, "A Nonlinear Field Theory of Deformable Dielectrics," *J. Mech. Phys. Solids*, **56**(2), pp. 467–486.
- [36] Toupin, R. A., 1962, "Elastic Materials With Couple-Stresses," *Arch. Ration. Mech. Anal.*, **11**(1), pp. 385–414.
- [37] Koiter, W. T., 1964, "Couple-Stresses in the Theory of Elasticity," *Proc. K. Ned. Akad. Wet., Ser. B Phys. Sci.*, **67**, pp. 17–44.
- [38] Mindlin, R. D., and Eshel, N. N., 1968, "On First Strain-Gradient Theories in Linear Elasticity," *Int. J. Solids. Struct.*, **4**(6), pp. 637–642.
- [39] Mindlin, R. D., 1964, "Micro-Structure in Linear Elasticity," *Arch. Ration. Mech. Anal.*, **16**(1), pp. 51–78.
- [40] Mindlin, R. D., and Tiersten, H. F., 1962, "Effects of Couple-Stresses in Linear Elasticity," *Arch. Ration. Mech. Anal.*, **11**(1), pp. 415–448.
- [41] Aifantis, E. C., 1984, "On the Microstructural Origin of Certain Inelastic Models," *ASME J. Eng. Mater. Technol.*, **106**(4), pp. 326–330.
- [42] Aifantis, E. C., 1992, "On the Role of Gradients in the Localization of Deformation and Fracture," *Int. J. Eng. Sci.*, **30**(10), pp. 1279–1299.
- [43] Fleck, N. A., and Hutchinson, J. W., 1997, "Strain Gradient Plasticity," *Adv. Appl. Mech.*, **33**, pp. 295–361.

- [44] Fleck, N. A., Muller, G. M., Ashby, M. F., and Hutchinson, J. W., 1994, "Strain Gradient Plasticity: Theory and Experiment," *Acta Metall. Mater.*, **42**(2), pp. 475–487.
- [45] Yang, F., Chong, A. C. M., Lam, D. C. C., and Tong, P., 2002, "Couple Stress Based Strain Gradient Theory for Elasticity," *Int. J. Solids and Struct.*, **39**(10), pp. 2731–2743.
- [46] Hadesfandiari, A. R., and Dargush, G. F., 2011, "Couple Stress Theory for Solids," *Int. J. Solids. Struct.*, **48**(18), pp. 2496–2510.
- [47] Maranganti, R., Sharma, N. D., and Sharma, P., 2006, "Electromechanical Coupling in Nonpiezoelectric Materials Due to Nanoscale Nonlocal Size Effects: Green's Function Solutions and Embedded Inclusions," *Phys. Rev. B*, **74**(1), p. 14110.
- [48] Aravas, N., 2011, "Plane-Strain Problems for a Class of Gradient Elasticity Models—A Stress Function Approach," *J. Elast.*, **104**(1–2), pp. 45–70.
- [49] Gao, X.-L., and Park, S., 2007, "Variational Formulation of a Simplified Strain Gradient Elasticity Theory and Its Application to a Pressurized Thick-Walled Cylinder Problem," *Int. J. Solids Struct.*, **44**(2223), pp. 7486–7499.
- [50] Toupin, R. A., 1956, "The Elastic Dielectric," *J. Ration. Mech. Anal.*, **5**, pp. 849–914.
- [51] Yang, J., 2005, *An Introduction to the Theory of Piezoelectricity*, Springer, New York.
- [52] Shu, L., Wei, X., Pang, T., Yao, X., and Wang, C., 2011, "Symmetry of Flexoelectric Coefficients in Crystalline Medium," *J. Appl. Phys.*, **110**(10), p. 104106.
- [53] Yang, J., Zhou, H., and Li, J., 2006, "Electric Field Gradient Effects in An Anti-Plane Circular Inclusion in Polarized Ceramics," *Proc. R. Soc. A*, **462**(2076), pp. 3511–3522.
- [54] Nowacki, J. P., 2006, *Static and Dynamic Coupled Fields in Bodies With Piezoeffects or Polarization Gradient*, Springer-Verlag, Berlin.